Fusion Engineering and Design 125 (2017) 71–76

Contents lists available at ScienceDirect

Fusion Engineering and Design

journal homepage: www.elsevier.com/locate/fusengdes

Digital twin applications for the JET divertor

D. Iglesias[a,*], P. Bunting[a], S. Esquembri[b], J. Hollocombe[a], S. Silburn[a], L. Vitton-Mea[c], I. Balboa[a], A. Huber[d], G.F. Matthews[a], V. Riccardo[a], F. Rimini[a], D. Valcarcel[a]

[a] UKAEA-CCFE, Culham Science Centre, Abingdon, Oxon OX14 3DB, UK
[b] UPM-I2A2, Technical University of Madrid, 28031 Madrid, Spain
[c] École Nationale Suprieure de Physique, Électronique et Matériaux (Phelma), Institut polytechnique de Grenoble Alpes, Grenoble, France
[d] Institute of Energy and Climate Research – Plasma Physics, Forschungszentrum Jülich, EURATOM Association, Trilateral Euregio Cluster, D-52425 Jülich, Germany

ARTICLE INFO

Keywords:
JET
Divertor
Thermal analysis
Tokamak operations
Real-time protection

ABSTRACT

Digital twin techniques enhance traditional engineering analysis workflows of existing systems when a realistic evaluation of a component under complex operating conditions is required. During preparation, commissioning and operating phases, components can be virtually tested by using validated numerical models, operational expertise, and experimental databases.

Three complementary applications have been developed under this approach. The numerical models used for the divertor tiles are based on continuum mechanics formulations. Their loading conditions are defined using the current physics and engineering understanding of a combination of experimental measurements. The aim of these tools is to increase operational range, reliability, and predictability of the JET divertor.

1. Introduction and requirements

JET is being enhanced for a second D-T operations campaign, which will push the limits of ITER-like Wall (ILW) components [1], and will also pose a challenge for diagnostic systems. A set of tools are in development with the objective of mitigating risks related to the unavailability or unreliability of protection IR cameras. In addition, increased accuracy will be provided to the understanding and the interpretation of these experiments.

The basic requirements for the new codes are grouped, as shown in Fig. 1, depending on the operating phase:

- Pulse preparation: The use of virtual modelling in this stage is to have a better estimate of the effect of the pulse in order to comply to the JET Operating Instructions (JOIs).
- Pulse monitoring: Real-time temperature estimation need reliable 2D nonlinear diffusion models.
- Post-pulse processing: Virtual Thermal Map (VTM) uses protection IR cameras. A backup for recreating the surface and bulk temperatures shall be provided through quick analysis.
- Condition and design assessment: any change on divertor components needs to be checked to actual experimental conditions, in order to evaluate the impact of any deviation from nominal geometry and properties, or even to assess new designs.

All of the previous simulation scenarios are the responsibility of different experts who do not necessarily have numerical analysis experience.

2. Objectives, formulation and models

In order to provide the functionality needed, each of the tools tackles one specific phase. As opposed to a typical analysis workflow, the main objective is maximizing the final user's productivity. Their design therefore hides any numerical complexity, and allows their operation using machine and experimental parameters. Several models are provided as a black-box, which is previously validated by analyst experts, but its source code can be inspected, audited, and extended at any time.

The formulation used for this first implementation is based on the thermal equilibrium using the Principle of Virtual Power. The contributions to the power virtual variation, $\delta\dot{\Pi}$, are calculated from the numerical integration of the following residual equation:

$$\delta\dot{\Pi} = \delta\dot{\Pi}_{\text{capacitance}} - \delta\dot{\Pi}_{\text{external}} - \delta\dot{\Pi}_{\text{conduction}} = 0 \tag{1}$$

Each of the previous contribution terms can be expressed in the reference configuration [2] as:

$$\delta\dot{\Pi}_{\text{capacitance}} = \int_{\mathscr{B}} \rho c_p \frac{\mathrm{dT}}{\mathrm{dt}} \delta T \ \mathrm{dV} \tag{2}$$

* Corresponding author.
E-mail addresses: diglesias78@gmail.com, daniel.iglesias@ukaea.uk (D. Iglesias).

http://dx.doi.org/10.1016/j.fusengdes.2017.10.012
Received 17 February 2017; Received in revised form 24 September 2017; Accepted 17 October 2017

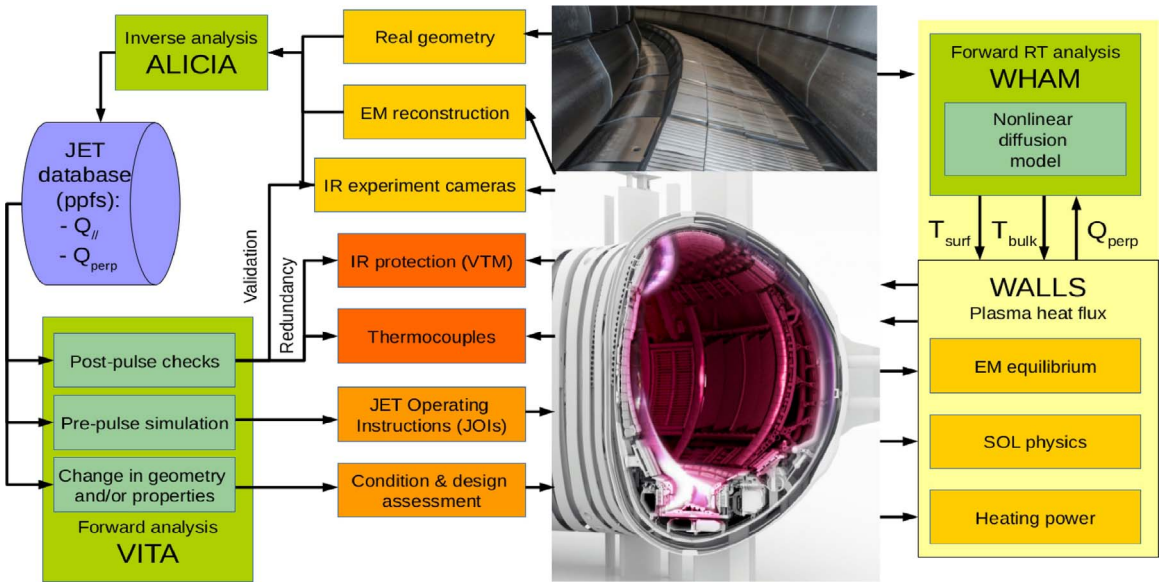

Fig. 1. Overall workflow scheme.

$$\delta\dot{\Pi}_{\text{external}} = \int_{\partial\mathscr{B}} \boldsymbol{q}\delta T\cdot\boldsymbol{n}\ \mathrm{dS} \tag{3}$$

$$\delta\dot{\Pi}_{\text{conduction}} = \int_{\mathscr{B}} (\boldsymbol{\kappa}\nabla T)\cdot\nabla\delta T\ \mathrm{dV} \tag{4}$$

where the conductivity tensor $\boldsymbol{\kappa}$ and the specific heat capacity c_p, are temperature dependent, $f(T)$, properties of the material. The density ρ is considered constant.

Fully nonlinear finite element (FE) approximations are used for all analyses, with some Galerkin meshfree enhancements [3] when applicable. Several de-featuring levels are applied when speed is a concern. Initial implementation uses 2D models shown in Fig. 2, but design is extensible to 3D in the future. Orthotropic effects, as well as Planck radiation or convection cooling are also foreseen.

Coatings and deposits can be modelled with exact properties, by means of a proper layer formulation which is available for all the applications. Usual parameters for the JET divertor tiles range from 10 to 20 μm thickness for the W coating on CFC tiles, to 50 μm node separation in direction normal to the surface for modelling ELMs accurately in bulk W tiles.

3. ALICIA

The *Augmented Lagrangian Implicit Constrained Inverse Analysis* tool uses the measured IR temperatures of the divertor tiles to compute the incoming heat flux density over time. Execution parameters correspond to the component's physical properties, and IR system characteristics (typically 9 kHz and 1.7 mm pixel width).

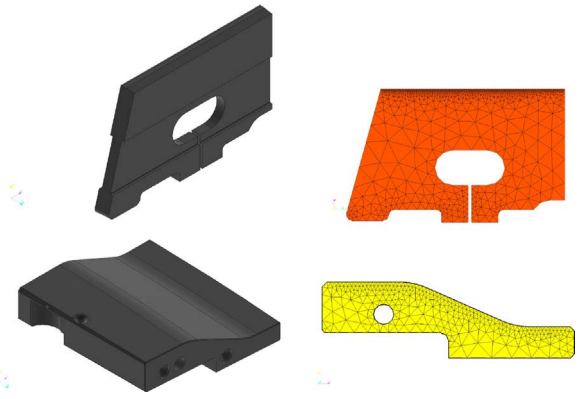

Fig. 2. 3D CAD (left) and 2D numerical discretization (right) of divertor components: tile 5 (top) and tile 6 (bottom).

The IR temperature measurements in Tungsten surfaces [4] are applied to the numerical model as a constrained Dirichlet boundary condition. In general, this is accomplished by adding a new term to Eq. (1). Existing inverse codes used for Fusion devices such as THEODOR [5], TACO [6], and QFLUX_2D [7] add a constraint equation in the form of $q_s = \alpha\Delta T$, which is interpreted as a deposited layer without any thermal capacity [8]. This term is not needed for the ILW and if considered would be in fact equivalent to a penalty method, which stores energy proportional to a numerical temperature difference, ΔT, in a similar way to a spring. The augmented Lagrangian scheme detailed in [2] adds a loop to the numerical procedure reducing the temperature difference until it is very small, $\Delta T < \epsilon$. This imposes the constraint without modifying the power balance, therefore increasing the accuracy.

The use of explicit integration schemes is also common in these types of analysis codes, as they usually need to be run between machine pulses. This scheme speeds up the solution at least by an order of magnitude. The faster explicit procedure has though two compromising features: the nonlinear properties can only be estimated as a parabolic function [5], and the size of the grid or mesh used for the geometrical model is limited by the CFL condition [9]. The use of an implicit scheme is not as fast but eliminates these limits, allowing the use of complex functions for the temperature dependent material properties, usually defined by experimental tables. More importantly, extremely fine meshes can be used at the surface improving the measurement of the intense gradients produced by fast transients. The extra computation effort is achieved in ALICIA through parallel multi-threaded execution.

The resulting output shows a much better capture of extremely fast events, such as filaments and ELMs. Fig. 3 compares the present version of THEODOR [10] used at JET-ILW (using a very high value for $\alpha = 1.44 \times 10^{15}\ \mathrm{W/m^2\,K}$) with the new code ALICIA specifically designed for the ILW. The test is carried out using a synthetic IR signal; generated by forward analysis using ANSYS modelling a bulk Tungsten tile with an extremely fine mesh. This difference has been consistently found using experimental IR measurements. In the case of W-coated CFC targets, the exact modelling of the coating layers—with thickness of 10–20 μm—improves the ELM peak heat flux measurement even more. Fig. 4 compares the two codes developed for JET divertor for tile 6, showing peak value differences of up to 100% for which only ALICIA gives ELM heat fluxes similar to those calculated for bulk-W tiles. The

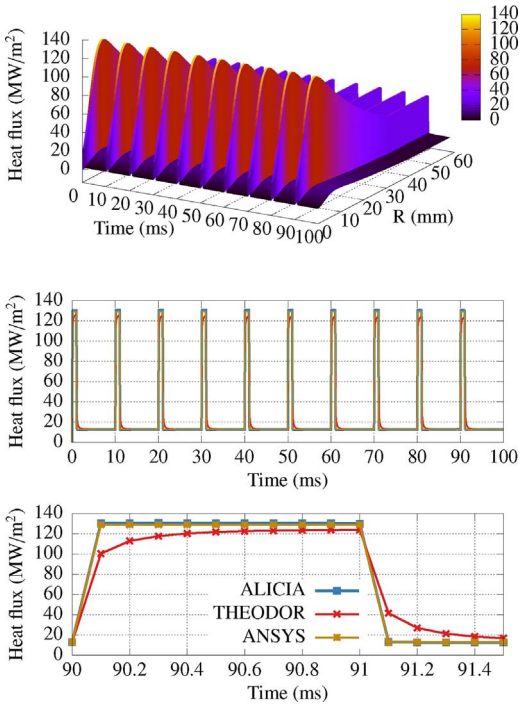

Fig. 3. Transient benchmark using ANSYS for generating the synthetic temperatures from the reference load. ALICIA output (top), and comparison between ALICIA and THEODOR peak heat flux (mid, bottom).

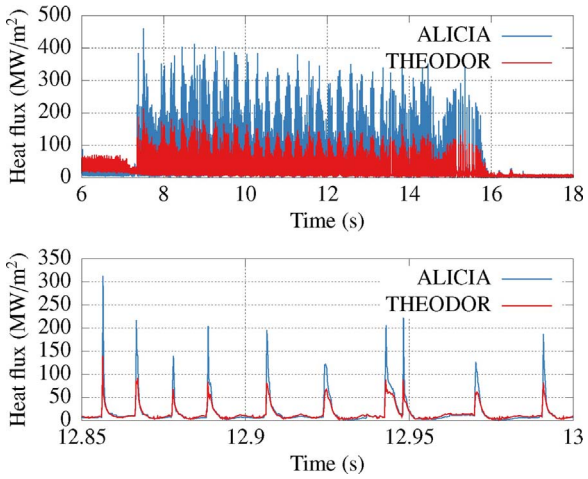

Fig. 4. H-mode pulse (JPN 90271): calculated maximum heat flux with THEODOR and ALICIA (top) with detail of ELM transients (bottom).

augmented Lagrangian scheme along with the refined mesh towards the plasma facing surface not only allows an almost perfect match of the varying load, but at the same time it also reduces the numerical noise, as shown in Fig. 5 for L-mode reconstruction comparison using real JET data.

In summary, the unique combination of numerical methods have shown to improve the existing heat flux calculation capabilities for the JET divertor in the following aspects:

- Augmented Lagrangian approach ensures temperature controlled smooth convergence and minimizes signal noise.
- An implicit integration scheme eliminates the numerical limits on element size, and enables any function definition for the nonlinear material properties.
- Finite element meshes allow modelling of irregular geometries.
- Multiple materials with layer simulation based on thickness, heat capacity and conductivity parameters are available for W-coated CFC tiles.

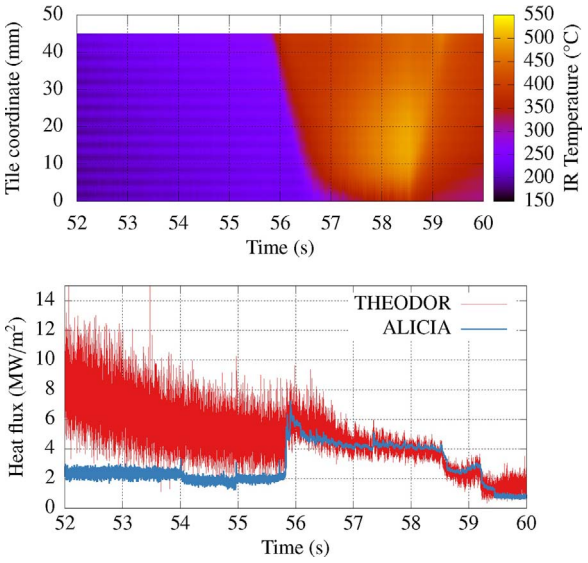

Fig. 5. L-mode pulse (JPN 89162): temperature measurement (top), and calculated maximum heat flux with THEODOR and ALICIA (bottom).

4. VITA

Virtual Thermal Assessments is a forward simulation code featuring a GUI—shown in Fig. 6—for ease of use. Its main goal is to allow both quick and accurate analysis of divertor tiles to users by setting global machine parameters, recreating previous stored pulses, or a mix of both. The time varying boundary conditions and integration parameters are automatically set, therefore not requiring the user to deal with numerical details.

It is designed for pulse preparation activities, post-pulse checks, and integrity assessments of damaged components. It may also be used to test alternative divertor configurations under experimental conditions. It includes the following capabilities:

- Several ways for defining pulse parameters—manually, or reading them from files or stored signals—and automatic setting of boundary conditions.
- Connection to the JET database for the readout of experimental measurements.
- Selection of the divertor tile and accuracy of the approximation.
- Direct plotting of diagnostic synthetic signals.
- Tabulated output of maximum temperature at the surface and thermocouple measurement points, along with energy values.

The parameters that define the pulse can be grouped as follows:Input power parametersThe total power input to the plasma arrives from either resistive heating, NBI or RF sources. Each of the three signals can be defined as a constant value or a table from a file allowing complex manual load inputs. In the case where an experimental pulse is to be recreated, each of these values can be read from their corresponding signal in the JET database.Plasma parametersThe total power arriving to the divertor at any moment in time corresponds to the total input minus the radiated power. This is taken into account as a factor in the range [0–1] called the radiated fraction. The outboard-inboard power ratio is estimated as 1/3 inboard, 2/3 outboard, and the footprint can be defined using three different functions:

- A triangular function is the simplest way of defining the shape when little information is known in advance of the simulation. Only the

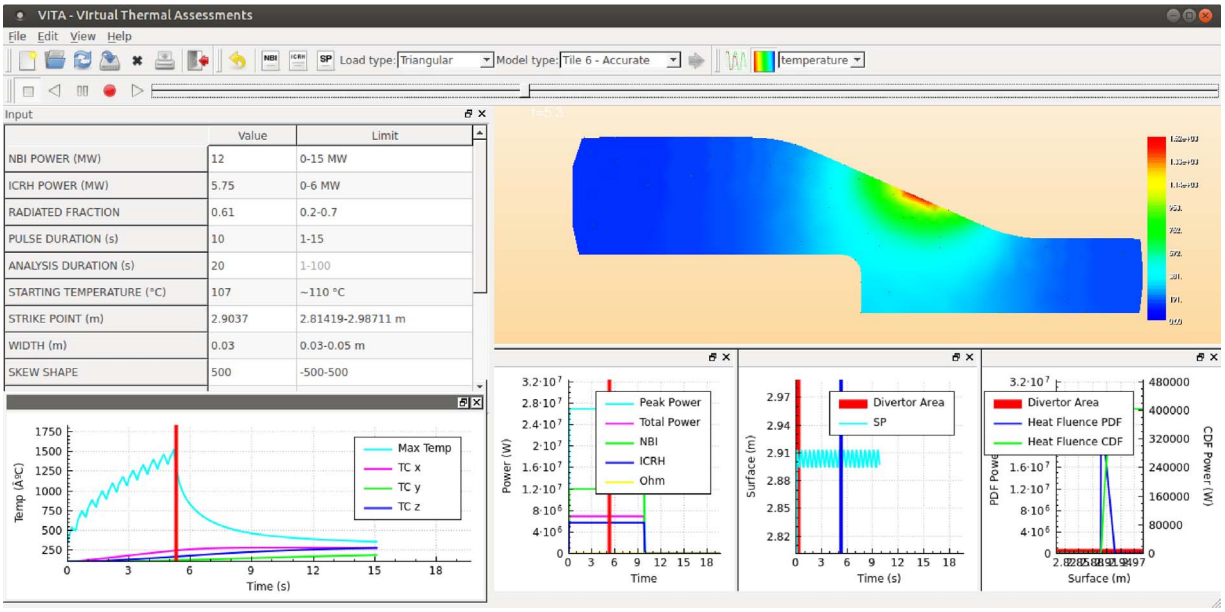

Fig. 6. VITA user's interface during tile 6 sweeping simulation.

width is needed for defining the footprint, allowing for a rough estimation of the bulk temperature evolution.

- A skewed Gaussian is a used as compromise between accuracy on the estimated footprint and speed. It is defined by its width and skewness values.
- The convolution of an exponential with a Gaussian has been proven in [11] to be the best fit to the experimental observations. This function defines the profile of the scrape-off layer (SOL) at the equatorial plane. The parameters defining this function correspond to the power fall-off width, λ, and the spreading factor, *S*. Their values can be manually fixed or estimated—as defined in [12]—as a function of the plasma current, I_p, toroidal field, B_t, integrated density, n_e, SOL power, P_{SOL}, ELM frequency, f_{ELM}, and the standard deviation of the radial field current, σ_{RF}.

Magnetic parametersIn the latter case, the power density needs to be projected from the equatorial to the divertor plane. By default the flux expansion is used, but an option is available for performing a 3D magnetic projection using the magnetic field components and the equilibrium reconstruction provided by the Flush code [13] at each calculation time step. A second option allows the magnetic shadowing of the surrounding tiles to be taken into account.The strike point position can be defined manually as a fixed location, or a regular sweep across it. It is also possible to input its evolution as a table or read it directly from an stored signal in the experimental database.Analysis parametersOnce the physical quantities which define the loading conditions have been set, the Diritchlet boundary conditions are automatically defined in the model. The power density footprint is combined with the strike point time evolution, defining the power at each boundary point. The use of analytical functions for the heat flux profile allows calculating the exact power density at every surface node in an energy consistent manner (i.e. eliminating interpolation errors). In addition, the application of meshfree C^{∞} shape functions greatly increases the accuracy of surface temperature simulation. In the case where the loading parameters have been manually specified, the duration of the heating stage can be defined by the pulse time. Finally, the total simulation time is input using the analysis duration parameter.

The accuracy of VITA has been tested to experimental data with satisfactory results. Fig. 7 compares the response of two H-mode medium and high power pulses with the IR camera signal used for experiment data analysis, which is much more accurate than the ones

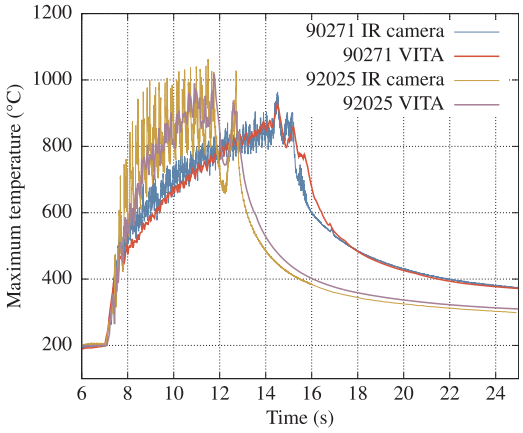

Fig. 7. VITA synthetic reconstruction of maximum temperature IR signal compared to experiment IR camera measurement for two H-mode pulses with medium (90271), and high power (92025) input power.

used for the protection of the JET-ILW [14]. Due to the large number of signals used for recreating the loading conditions, there is of course an overall associated uncertainty. The total error has been bounded to 10% of the measured temperatures, being comparable to the mismatch observed between the machine protection and experimental camera systems. The differences in amplitude during the sweeping of the strike point position is mostly due to the IR being measured in a tile extension instead of the full length tile. This short extension has a local shadow which amplifies the temperature oscillations. During the upcoming campaign, a normal length tile will be diagnosed. This will allow the specific testing of VITA against the alarms of the protection system. As the oscillation of the IR will be reduced, and the alarms are set to trigger when 200 ms overheating events are detected [15]—in line with the response time of VITA models—lower errors are expected.

5. WHAM

WALLS Heat Analysis Module is the first nonlinear thermal finite element solver designed to work in a tokamak real time machine protection system. It is included as a module for the wall load limitation system (WALLS) [16], simulating the transient 2D thermal response of plasma facing components.

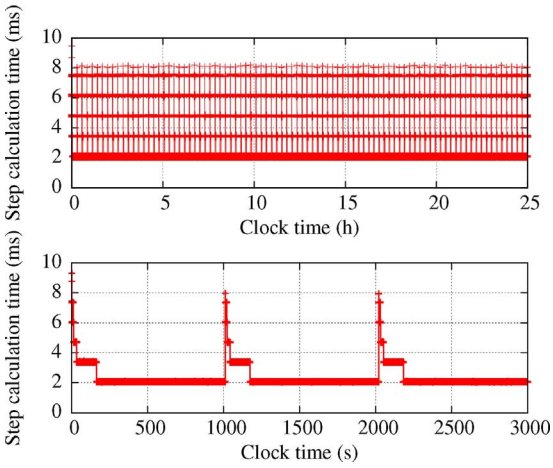

Fig. 8. Stability analysis for WHAM (top), with detail (bottom).

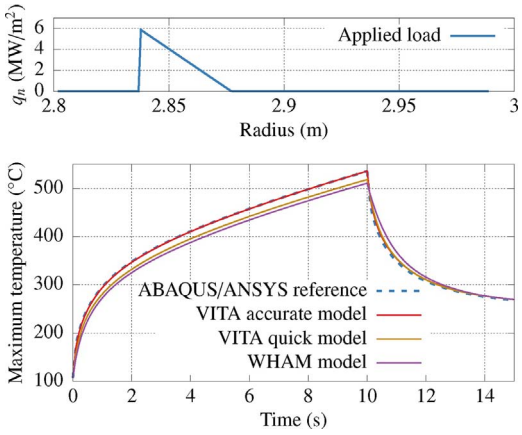

Fig. 9. Numerical validation for a triangular heat flux density profile q_n (top) applied as a stepped load for 10 s, showing less than 8% error between WHAM and ANSYS/VITA reference solutions (bottom).

The module is initialized by the definition of the model geometry and properties, and the boundary interface nodes. The WALLS system directly computes the value for the total power at each node, which is an input to WHAM at each time step. There is also a function for resetting the model's temperatures to a value (e.g. thermocouples measurement) right before the beginning of each pulse.

The operational requirements impose that it must output the synthetic tile surface temperatures within a strict cycle time limit of 8.5 ms. In addition, the module should operate continuously for months without any external intervention. This is due to the whole real-time platform being deployed at the start of the campaign, and operated without interruption, as rebooting the whole system is a time consuming process that would lead to delays in operation. Successful tests have been performed to comply with these operational requirements, as shown in Fig. 8.

The short time available for solving each time step implies a reduction on the size of the underlying mesh. An initial comparison of the numerical accuracy has been performed between the ABAQUS/ANSYS reference solution, two VITA models, and WHAM. A sharp triangular load has been used as a worst case for the radial footprint, applied as a time stepped function. Fig. 9 shows that the intrinsic error of the WHAM reduced model is not much more to that of the quick VITA model, within 5–8% of the almost exact solution provided by the VITA accurate model. The test also reveals that the dynamic response of this model is slower, but good enough to capture the bulk behaviour of the tile.

The performance of WHAM has been evaluated within a high power

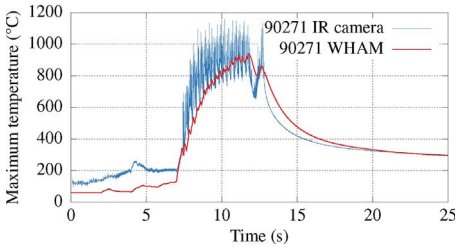

Fig. 10. WHAM maximum temperature real-time simulation compared to IR camera measurement for a high power H-mode pulse (92025).

swept pulse in Fig. 10. The maximum temperature evolution of the model is compared to the fast IR experiment camera signal, with good agreement for the evolution of the temperatures. The error once the ELMs temperatures are removed is estimated to be 15%. Cooling down is also well captured, demonstrating that the whole energy in the tile is properly calculated. These satisfactory results show that the WHAM temperature output can be used as a protection signal for the JET-ILW divertor.

6. Conclusions and further work

Three complimentary applications have been introduced for enhancing JET divertor operations using a digital twin approach. All of them have been verified using commercial codes (Abaqus, ANSYS), extensively validated to experimental data, and can be executed exclusively using machine parameters, diagnostics characteristics, and material properties. The use of modern C++11 language maximizes execution speed and maintainability of the codes.

The final goal is increasing the JET reliability, operational limits, and accuracy of experimental results. Pulse preparation, IR diagnostics fallback, and real-time protection systems have been enhanced by this first implementation. This work will be continued using user and final customer's feedback, and application to other in-vessel components and machines will follow.

Acknowledgements

This work has been carried out within the framework of the Contract for the Operation of the JET Facilities and has received funding from the European Union's Horizon 2020 research and innovation programme. The views and opinions expressed herein do not necessarily reflect those of the European Commission.

References

[1] G.F. Matthews, et al., JET ITER-like wall – overview and experimental programme, Phys. Scr. T145 (2011) 014001.
[2] D. Iglesias, On the application of meshfree methods to the nonlinear dynamics of multibody systems (Ph.D. Thesis), Universidad Politécnica de Madrid, 2016, http://dx.doi.org/10.20868/UPM.thesis.39121.
[3] D. Iglesias, et al., Application of Galerkin meshfree methods to nonlinear thermo-mechanical simulation of solids under extremely high pulsed loading, Fusion Eng. Des. 88 (9–10) (2013) 2744–2747.
[4] I. Balboa, et al., Upgrade of the infrared camera diagnostics for the JET ITER-like wall divertor, Rev. Sci. Instrum. 83 (2012) 10D530.
[5] A. Herrmann, et al., Energy flux to the ASDEX-Upgrade diverter plates determined by thermography and calorimetry, Plasma Phys. Controll. Fusion 37 (1995) 17.
[6] K.F. Gan, et al., 2D divertor heat flux distribution using a 3D heat conduction solver in National Spherical Torus Experiment, Rev. Sci. Instrum. 84 (2013) 023505.
[7] B. LaBombard, et al., Divertor heat flux footprints in EDA H-mode discharges on Alcator C-Mod, J. Nucl. Mater. 415 (1) (2013) S349–S352.
[8] A. Herrmann, Limitations for divertor heat flux calculations of fast events in tokamaks, Proc. 28th EPS Conf. on Controlled Fusion and Plasma Physics (2001).
[9] R. Courant, et al., On the partial difference equations of mathematical physics, IBM J. Res. Dev. 11 (2) (1967) 215–234.
[10] B. Sieglin, et al., Real time capable infrared thermography for ASDEX Upgrade, Rev. Sci. Instrum. 86 (2015) 113502.
[11] T. Eich, et al., Scaling of the tokamak near the scrape-off layer H-mode power width and implications for ITER, J. Nucl. Mater. 438 (2013) S72–S77.

[12] V. Riccardo, et al., Power footprint definition for JET divertor protection, 22nd International Conference on Plasma Surface Interactions in Controlled Fusion Devices, PSI 22 (2016).
[13] S. Pamella, et al., Improvements to the flux surface handling code FLUSH, EUROfusion WPJET1PR(15)05 (2015) Preprint of Paper to be submitted for publication in Fusion Engineering and Design.
[14] M. Jouve, et al., Real-time protection of the 'ITER-like wall at JET', Contribution to the Proceedings of the 13th ICALEPCS (2012) 1118–1121 ISSN 2226-0358.
[15] G. Arnoux, et al., A protection system for the JET ITER-like wall based on imaging diagnostics, Rev. Sci. Instrum. 83 (10) (2012) 10D727.
[16] D. Valcarcel, et al., The JET real-time plasma-wall load monitoring system, Fusion Eng. Des. 8 (3) (2013) 243–258.